Chapter 12

Biomethanol from Glycerol

Joost G. van Bennekom,
Robertus H. Venderbosch and Hero J. Heeres

Additional information is available at the end of the chapter

http://dx.doi.org/10.5772/53691

1. Introduction

Methanol is an important bulk chemical in the chemical industry. The global methanol demand was approximately 32 million metric tons in 2004 and is expected to grow [1]. Methanol is used mainly for the production of formaldehyde, acetic acid, and application products including polymers and paints. Furthermore, methanol can be used as a clean and renewable energy carrier [1]. Methanol is mainly produced from syngas, a mixture of H_2, CO, and minor quantities of CO_2 and CH_4. Syngas is commonly produced from fossil resources like natural gas or coal. Biomass, however, can also be used as resource for syngas and allows the synthesis of green methanol. Green methanol not only has environmental benefits, but may also lead to considerable variable cost reductions if the biomass resource has a low or even negative value.

1.1. Renewable methanol

Methanol synthesis from biomass was already proposed during the first oil crisis in the 1970s [1]. In the 1980s a comprehensive review was published on the production of methanol from syngas derived from wood. Different gasification technologies were proposed and demonstration projects of these technologies were discussed [2, 3]. In the mid 1990s several projects on methanol synthesis from biomass were initiated such as the Hynol project in the USA and the BLGMF (black liquor gasification with motor fuels production) process in Sweden [4-6]. Schwarze Pumpe, Germany developed a process to convert coal and waste, including sewage sludge, to methanol (capacity ± 150 ML/y) [7]. Unfortunately no experimental data of these processes are available in open literature.

Several initiatives were started in the 2000s. At a scale of 4 t/d, Chemrec in Sweden produces methanol and dimethyl ether (DME) since 2011. Syngas is obtained by entrained flow gasifi-

cation of black liquor [8]. The production of methanol from glycerol is demonstrated on industrial scale by BioMCN in The Netherlands [8]. At BioMCN, the natural gas reforming unit has been modified to enable steam reforming of glycerol. The syngas is converted to methanol in their conventional packed bed methanol synthesis reactors, with a capacity for methanol production of 250 ML/y [8].

The amount of published experimental results on the production of methanol from biomass is rather limited. Most publications on methanol production from biomass are desk-top studies and data comparison is difficult [5, 6, 9-13]. These studies often combine biomass gasification and conventional methanol synthesis with, in some cases, electricity production [5, 6, 11, 13]. Xu *et al.* conducted an experimental study and demonstrated methanol production from biomass by reforming pyrolysis liquids into H_2 and CO_2 followed by catalytic syngas conditioning to convert part of the CO_2 into CO [14]. Methanol synthesis was conducted in a packed bed reactor, with an overall carbon conversion of around 23% (corresponding with a methanol production rate of 1.3 kg methanol/kg catalyst/h).

An interesting concept of using biomass to produce methanol is the co-processing of biomass and fossil resources, e.g. co-gasification of biomass with coal or natural gas [9, 10, 12]. The advantage of co-feeding natural gas is that the syngas derived will become more suitable for methanol synthesis as syngas from biomass is deficient in H_2 and syngas from natural gas in CO or CO_2.

The concepts involved in the current processes for the synthesis of methanol from biomass generally involve an initial gasification step at elevated temperatures and pressures. The approach demonstrated in this chapter is syngas production through a hydrothermal process, viz. conversion of a wet biomass stream to syngas by reforming in supercritical water (RSCW), followed by high pressure methanol synthesis.

An interesting wet biomass resource is glycerol, the by-product from the biodiesel industry. In Europe, the share of transportation fuel to be derived from renewable resources in 2020 is targeted at 10% [15]. It is expected that biodiesel and ethanol will make up the largest share and consequently Europe's biodiesel production increased significantly in the 2000s (see Figure 1) [16]. In the last few years, though, economics of biodiesel production deteriorated as the income from the sales of glycerol decreased, while the costs of feedstock increased.

As for the production of every (metric) ton of biodiesel, roughly 100 kg of methanol is required and a similar quantity of glycerol is produced, both methanol demand and glycerol production increased. An interesting option addressing the surplus of glycerol and the demand for methanol is to produce methanol from the glycerol. If this process is conducted by the biodiesel producer he will become less dependent on the methanol spot price, there is a (partial) security of supply of methanol, and by-products can be used as a green and sustainable feed product. However, the scale of traditional methanol synthesis (> 2000 t/d) is much larger than the scale of methanol synthesis explored in the Supermethanol project.

http://dx.doi.org/10.5772/53691

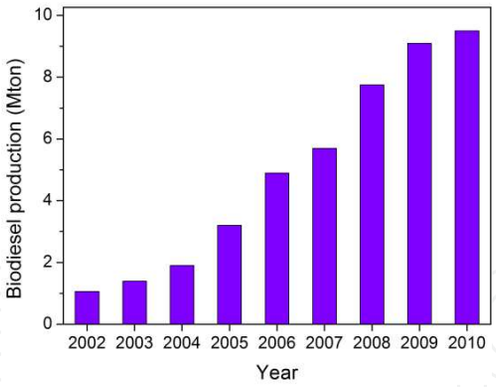

Figure 1. Biodiesel production in Europe. Adapted from reference [16].

The Supermethanol initiative focuses on a small/medium scale biodiesel plant (30,000 – 100,000 t/y) and the aim of the project is to develop a methanol synthesis process using glycerol as feed at a capacity matching the biodiesel production. The glycerol intake for the production of syngas will be in the range of 3000 up to 10,000 t/y [17]. The scope of the Supermethanol concept is schematically outlined in Figure 2.

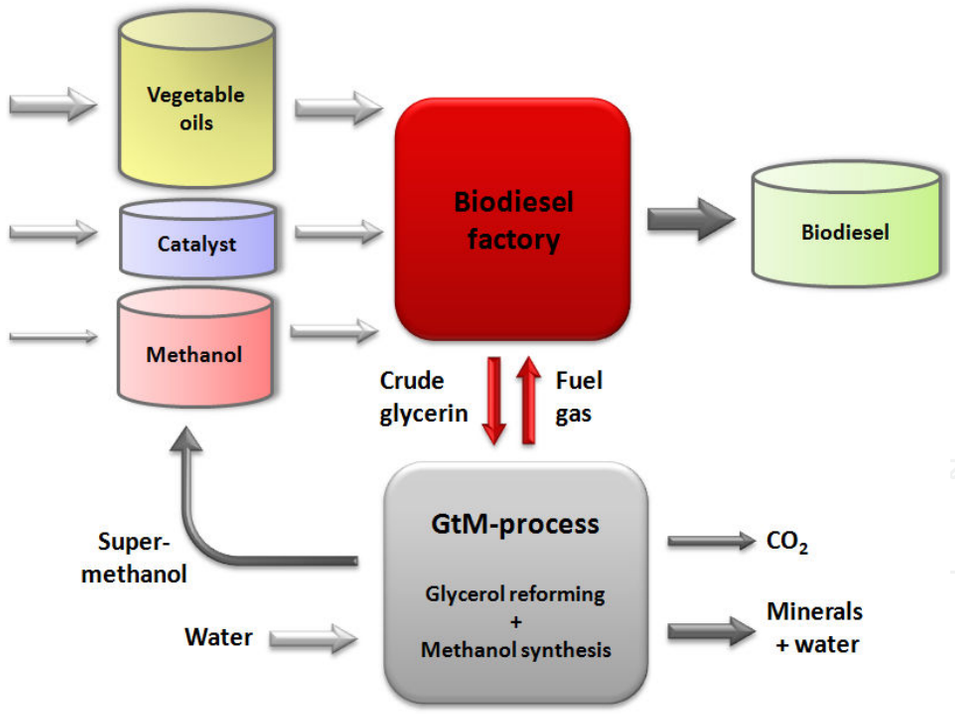

Figure 2. Outline of the Supermethanol concept. The glycerol-to-methanol (GtM-) process is the process under investigation in the Supermethanol project.

The biodiesel factory is the core of the process in which vegetable oils react with methanol in the presence of a catalyst to produce biodiesel and by-product glycerol. The glycerol can be converted into methanol in the glycerol-to-methanol (GtM-) process. This process is an inte-

gration of two separate processes, viz. the reforming in supercritical water (RSCW) of glycerol to syngas, followed by the conversion of this syngas into methanol. Additional fuel gas is produced, which can be used to generate heat for the biodiesel production or in the GtM-process. A more detailed overview on the GtM-concept is given in the next section.

2. The glycerol-to-methanol concept

2.1. Theoretical considerations

The most attractive syngas for methanol synthesis has a stoichiometric number (S_N), defined in Eq. 1, of approximately 2, which corresponds to the stoichiometric ratio for methanol synthesis.

$$S_N = \frac{\left(H_2 - CO_2\right)}{\left(CO + CO_2\right)} = 2 \tag{1}$$

When glycerol decomposes solely into H_2, CO, and CO_2 the maximum S_N is 1.33. This is illustrated by Eqs. 2 and 3. In Eq. 2, glycerol decomposition into syngas including the reversible water-gas shift (WGS) reaction is given. The syngas composition at equilibrium (neglecting methanation), expressed in terms of x, is a function of the temperature and the water concentration.

$$C_3H_8O_3 \xrightarrow{xH_2O} \left(3\text{-}x\right)\ CO + \left(4\text{+}x\right)\ H_2 + x\ CO_2 \tag{2}$$

Application of the definition for S_N and introduction of gas phase compositions in terms of x (see Eq. 3) confirms that the S_N value is 1.33 at most and independent of the progress of the WGS reaction:

$$S_N = \frac{\left(H_2 - CO_2\right)}{\left(CO + CO_2\right)} = \frac{\left(4 + x - x\right)}{\left(3 - x + x\right)} = \frac{4}{3} \tag{3}$$

The S_N value, though, can be increased by the addition of H_2 to, or removal of CO_2 from, the syngas. To obtain the highest methanol yield per kg glycerol, glycerol reforming followed by syngas conversion should proceed, for example, according to Eq. 4, where glycerol is selectively converted into H_2, CO, and CO_2. Subsequently, all H_2 and CO react to methanol, while the CO_2 remains.

$$3\ C_3H_8O_3 + 2\ H_2O \rightarrow 7\ CO + 14\ H_2 + 2\ CO_2 \rightarrow 7\ CH_3OH + 2\ CO_2 \tag{4}$$

As a theoretical maximum, 2.33 mol carbon/mol glycerol end up in methanol (77.8% on carbon basis or 0.81 kg methanol/kg glycerol on weight basis). Actual yields, however, will be lower as both processes, glycerol reforming and methanol synthesis, involve equilibrium reactions and the occurrence of other reactions like the formation of higher hydrocarbons, higher alcohols (HA), and methanation.

2.2. Description of the continuous integrated GtM-bench scale unit

The integrated unit consists of a reformer section and a methanol synthesis section. A schematic flow sheet of the unit is given in Figure 3. An extensive description of the reformer section is published elsewhere [18]. The reformer section was operated in continuous mode with a throughput of 1 L aqueous feed/h. Glycerol and water were introduced to the system from feed containers F1 or F2 through a pump and subsequently reformed in five reforming reactors (R1 – R5) in series. The temperature in each reactor can be adjusted individually.

During operation *in situ* separation of the water and gas phase after the reformer section was performed in a high pressure separator (HPS). The liquid phase in the HPS, can either be depressurized and transferred to a low pressure separator (LPS) or recycled via a recycle pump. In the former operating mode (using the LPS), the gases dissolved in the aqueous phase are released, quantified (Gallus G1.6 gas meter), and analyzed (gas chromatography, GC). In the latter operation mode (recycle mode) the gases remain dissolved and fresh glycerol feed is injected in the recycle stream before the first reforming reactor (R1). If required all reforming reactors can easily be filled with catalyst. The gas phase from the HPS was directly fed to the methanol synthesis section without upgrading or selective removal of components.

The methanol section contains three tubular packed bed reactors (P1 – P3, each L = 500 mm, ID = 10 mm) surrounded by heating jackets. A heating/cooling medium was flown through the heating jackets to control the temperature in the reactors. Temperatures were recorded at 4 positions inside packed bed P2 (at locations 2 to 30 cm from the entrance) and at the exit of packed bed reactors P2 and P3. Two or three of the tubular reactors were filled with catalyst particles ($1 < d_p < 3$ mm). The mixture of methanol, water, and unconverted gases leaving the last packed bed (P3) was cooled (cooler C2) using tap water, depressurized and cooled (cooler C3) to temperatures below 263 K to trap all condensables. Liquid samples were collected in a vessel and the unconverted gas was quantified (Gallus G1.6 gas meter) and analyzed by GC. The methanol synthesis reactors were operated at temperatures of the heating medium between 473 – 523 K and at similar pressure as the reformer section. Several process parameters were logged during operations and the locations, where they were measured, are indicated with letters in bold in Figure 3.

The process pressure was the average of $\mathbf{A}_{1\text{-}3}$, the temperature of reactor R5 (T_{R5}) was measured at **B** at the end of reactor R5, the glycerol feed flow at **C**, the gas flow of the HPS and LPS at $\mathbf{D}_1$ and $\mathbf{D}_2$ respectively, the temperature at the end of the methanol synthesis bed at **E**, the amount of liquid product at **F**, and the unconverted gas flow at **G**.

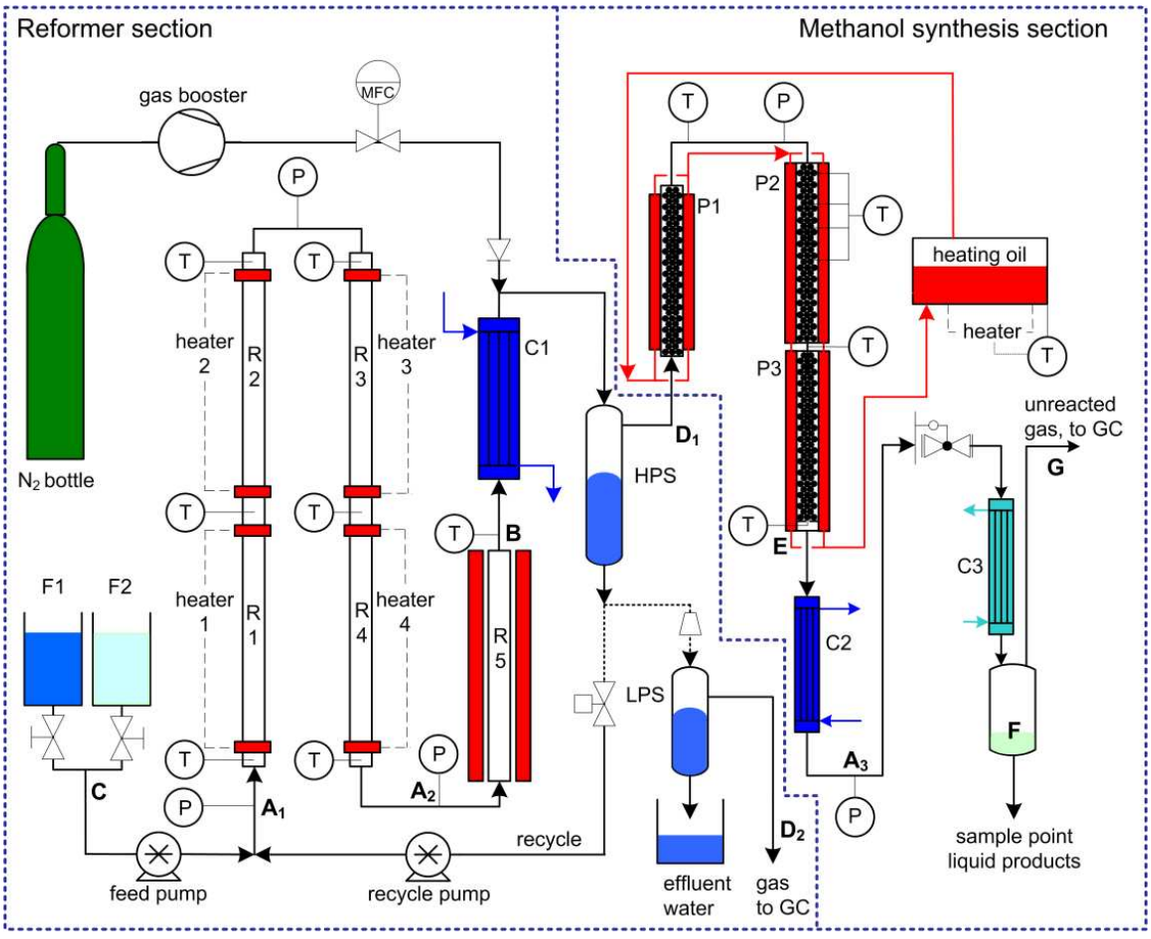

Figure 3. Flow sheet of the integrated GtM-bench scale unit. HPS and LPS refer to high pressure separator and low pressure separator respectively. F = feed container, C = cooler, P = packed bed reactor, R = reforming reactor. The bold capital letters correspond to the locations where relevant process parameters were measured [8].

2.3. Analyses

The composition of the off-gas from the reforming section and methanol synthesis section was analyzed using an online dual-column gas chromatograph (GC 955, Syntech Spectras) equipped with thermal conductivity detectors. CO was analyzed and quantified using a molsieve 5 Å column (L = 1.6 m) with helium as carrier gas. CH_4, CO_2, and C_{2+} were analyzed on a Chromosorb 102 column (L = 1.6 m) with helium as carrier gas. H_2 was analyzed on the molsieve column using argon as carrier gas. The total organic carbon (TOC) content of the effluent water from the RSCW process was analyzed using a TOC analyzer (TOC-V_{CSN}, Shimadzu). The water content of the methanol was determined by Karl Fischer-titration. The composition of the organics in the liquid phase after the methanol synthesis reactor was determined with a GC (HP 5890 series II) equipped with a flame ionization detector (FID) over a Restek RTX-1701 column (L = 60 m, ID = 0.25 mm) coupled with a mass spectrometer (MS, HP 5972 series). The FID was used for the quantification of the components and the MS for the identification of the components. The FID was calibrated for the main

constituents of the organic fraction: methanol, ethanol, 1-propanol, 2-propanol, 1-butanol, 2-butanol, 1-pentanol, 2-methyl-1-propanol, 2-methyl-1-butanol.

2.4. Definitions

The carbon conversion of glycerol (ζ_{gly}) in the reformer section is defined as the difference between the molar carbon flow of glycerol in the feed and the effluent ($\phi_{C,gly}$ - $\phi_{C,effluent}$) over the molar carbon flow of glycerol in the feed ($\phi_{C,gly}$):

$$\zeta_{gly} = \frac{\phi_{C,gly} - \phi_{C,effluent}}{\phi_{C,gly}} \cdot 100\% \tag{5}$$

The overall conversion of carbon in glycerol to carbon in methanol (ζ_C) in the integrated unit is the molar carbon flow in methanol ($\phi_{c,MeOH}$) over the molar carbon flow of glycerol in the feed.

$$\zeta_C = \frac{\phi_{C,MeOH}}{\phi_{C,gly}} \cdot 100\% \tag{6}$$

The methanol yield (η) is the mass flow of methanol (ϕ_{MeOH}) produced over the mass flow of glycerol (ϕ_{gly}) fed.

$$\eta = \frac{\phi_{MeOH}}{\phi_{gly}} \tag{7}$$

The conversion of gas component i (ζ_i) in methanol synthesis is defined as the molar conversion rate ($\phi_{i,in}$ - $\phi_{i,off}$) over the molar flow of component i originally present ($\phi_{i,in}$) after glycerol reforming.

$$\zeta_i = \frac{\phi_{i,in} - \phi_{i,off}}{\phi_{i,in}} \cdot 100\% \tag{8}$$

The carbon selectivity towards product i (σ_i) is defined as the molar carbon flow of product i ($\phi_{C,\,i,\,off}$) over the molar carbon flow of glycerol in the feed.

$$\sigma_i = \frac{\phi_{C,i,off}}{\phi_{C,gly}} \cdot 100\% \tag{9}$$

2.5. Research strategy

The integration of syngas production in an RSCW-process and syngas conversion in methanol synthesis is the core of the GtM-process. In the RSCW of glycerol a high pressure syngas is produced. The use of this high pressure syngas has distinct advantages for methanol synthesis, which will be dealt with in Section 4. However, before successful integration both processes need to be optimized separately, which was done at the laboratories of the Biomass Technology Group (BTG) in The Netherlands. A unit was available to investigate both process separately before integraton. Results obtained for each process were used to optimize the overall process and maximize the overall carbon conversion (ζ_C), which was the main focus of the research study on the integrated process.

3. Glycerol reforming in supercritical water

3.1. Introduction to reforming

Water becomes supercritical at conditions above its critical temperature (T_c = 647 K) and critical pressure (P_c = 22.1 MPa). In the phase diagram in Figure 4 the square area in the upper right corner represents the supercritical area of water [19].

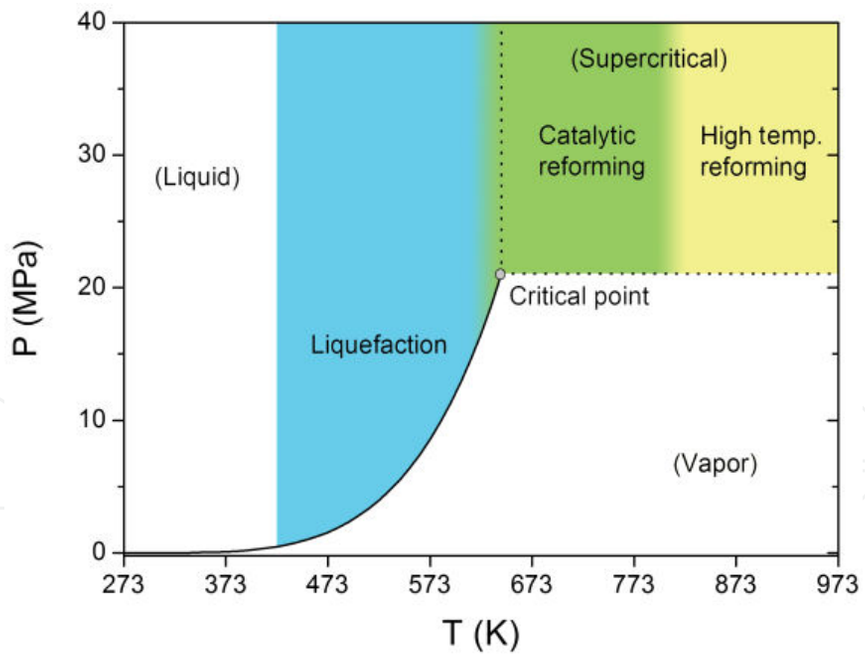

Figure 4. Phase diagram of water. Phases are indicated in parenthesis. Hydrothermal processes with their typical conditions are indicated in the colored areas. Adapted from reference [19].

Typical process conditions for three processes considered for wet biomass valorization are indicated here, viz. liquefaction, catalytic reforming, and high temperature reforming. Hydrothermal liquefaction is conducted at temperatures below and pressures above the critical

point, where biomass is degraded to yield mainly bio-crude (a viscous water-insoluble liquid), char, water-soluble substances, and gas [20]. RSCW of biomass is aimed at gas production and is carried out at conditions beyond the critical point. Here, water acts both as reaction medium and reactant. RSCW of biomass can be subdivided into catalytic reforming and noncatalytic reforming. Catalytic reforming is predominantly carried out at the lower temperature range, while noncatalytic or high temperature reforming is conducted at the higher temperatures (see Figure 4 [19]).

RSCW is characterized by the occurrence of many reactions, proceeding both in series and in parallel. The overall reaction of an actual (biomass) feed to liquid and gas phase products is shown in Eq. 10.

$$C_xH_yO_z + a\ H_2O \rightarrow \alpha\ CO + \beta\ H_2 + \gamma\ CO_2 + \delta\ H_2O + \varepsilon\ CH_4 + \eta\ C_{x'}H_{y'}O_{z'} \quad (10)$$

By-products ($C_{x'}H_{y'}O_{z'}$) are low molecular weight organic compounds, polymerized products, higher hydrocarbons ($x' \geq 2$, $z'=0$), or elemental carbon ($y'=z'=0$). Some of the low molecular weight organics can react further to gas phase components. Subsequent reactions of the gas phase components may also occur. The following gas phase reactions may occur, depending on process conditions [21]:

$$CO + H_2O \leftrightarrow CO_2 + H_2 \quad (11)$$

$$CO + 3\ H_2 \leftrightarrow CH_4 + H_2O \quad (12)$$

$$CO_2 + 4\ H_2 \leftrightarrow CH_4 + 2\ H_2O \quad (13)$$

$$2\ CO \leftrightarrow CO_2 + C \quad (14)$$

$$CH_4 \leftrightarrow C + 2\ H_2 \quad (15)$$

$$CO + H_2 \leftrightarrow C + H_2O \quad (16)$$

The individual reaction rates depend on operating conditions and the presence of catalysts. A number of parameters affect the carbon conversion in RSCW, such as feedstock type, feed concentration, operating conditions, presence of catalysts or catalytic surfaces, and interaction between different components. The state of the art of RSCW in the 2000s has been reviewed extensively in several publications [19, 22-28].

3.2. Reforming of pure glycerol and crude glycerin

The reforming experiments were carried out using only the reforming section of the unit depicted in Figure 3. Typical conditions were temperatures of 723 – 923 K, residence times between 6 – 45 s, and feed concentrations of 3 – 20 wt%. The pressure was around 25 MPa. Two different types of glycerol were used, viz. pure glycerol and crude glycerin. Crude glycerin is glycerol derived from biodiesel production. The crude glycerin used in this research study contains approximately 5 wt% NaCl. The presence of alkali (in this case Na^+) influences mainly the WGS reaction (see Eq. 11). The main gas products for pure glycerol and crude glycerin were: H_2, CO, CO_2, CH_4, and C_2H_6. At complete conversion, roughly 2 mol of carbon in glycerol are converted to carbon oxides while 1 mol of carbon ends up as a hydrocarbon. The gas composition/yield appeared to be a function of the conversion and independent of the feed concentration. The conversion is a function of the process severity, a combination of the residence time and operating temperature. In Figure 5 the gas yields (mol gas/mol glycerol) of the two types of glycerol are depicted. The trend lines shown are fitted to experimental data points [18]. The differences between pure glycerol and crude glycerin can be mainly attributed to the extent of the progress of the WGS reaction [18].

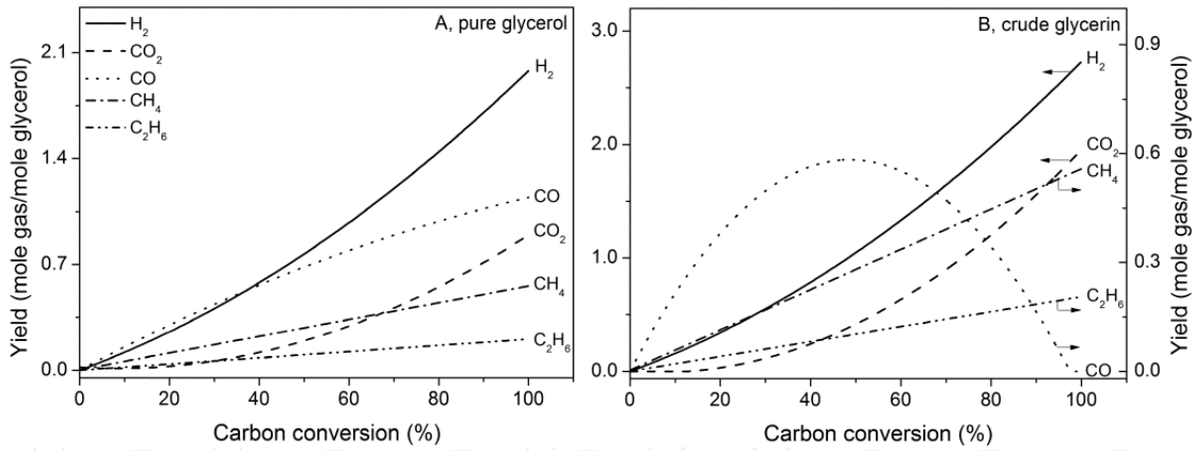

Figure 5. Relations between the conversion and the gas yield for pure glycerol (A) and crude glycerin (B) [29].

From reforming studies with methanol as model compound it was concluded that the hydrocarbons present in the gas mixture in case of glycerol reforming appear to be primary gas phase products. In the methanol reforming experiments in the same unit, gas mixtures with similar H_2, CO, and CO_2 ratios were obtained, but hydrocarbons were hardly observed. Thus, gas phase reactions producing hydrocarbons, e.g. methanation, hardly proceed in the system, which indicates that hydrocarbons are primary gas phase products formed upon glycerol decomposition and not or only to a small extent by gas phase reactions. In glycerol reforming the reactions depicted in Eqs. 10 and 11 proceed, while Eqs. 12 and 13 barely take place. Coke formation was not observed at all and most probably the reactions depicted in Eqs. 14-16 do not proceed.

http://dx.doi.org/10.5772/53691

Based on the experimental results, a simplified reaction scheme for the decomposition of glycerol with a focus on gas production was established and is given in Figure 6. More information on the selection of primary and secondary gas phase products can be found in literature [18].

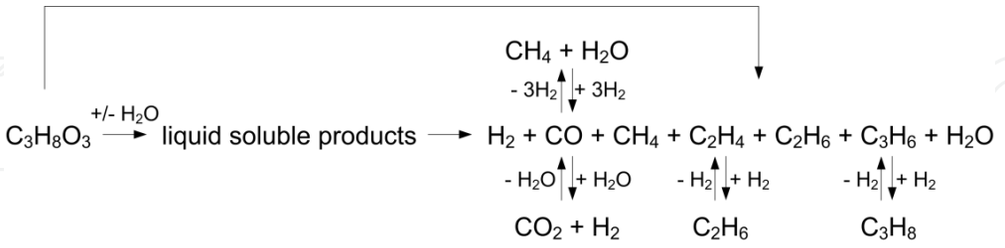

Figure 6. Decomposition pathways for glycerol in SCW to gaseous products including possible follow-up reactions [18].

In this scheme, CH_4 is shown as a primary product, but can also be formed as a secondary product by methanation. Furthermore, water is produced and the WGS reaction and alkene hydrogenation are included. It is suggested that glycerol can either decompose into liquid soluble products that react further to gas products or that glycerol can directly decompose into gas products. In practice probably both reaction pathways occur. The overall mechanism at complete conversion of glycerol decomposition proceeds through the dehydration of 1 mol H_2O/mol feed [18].

An important quality indicator for the gas composition is the S_N value as defined in Eq. 1. A S_N as close as possible to 2 is desired for methanol synthesis, but as was shown in Eq. 3 a S_N value of 1.33 is the maximum for gas derived in glycerol reforming. The experimental S_N as function of the glycerol conversion is depicted in Figure 7. It can be seen that for both types of glycerol the S_N decreases with increasing conversion. The values are almost equal up to 60%, but differ considerably at the higher conversion. The most attractive S_N's are obtained at the lower conversion although they remain below 1. The S_N can be improved by suppressing the formation of hydrocarbons, which is a challenge as hydrocarbons are formed as primary gas phase products.

3.3. Catalytic reforming

Catalytic reforming was investigated to improve the quality of the syngas obtained in the noncatalytic reforming experiments for subsequent methanol synthesis. An extensive description of catalytic reforming using five different catalysts is given in literature [29]. The catalytic experiments were conducted at temperatures between 648 to 973 K at pressures between 25.5 - 27.0 MPa. The feed concentration was 10 wt%, and the residence time varied from 8 to 87 s. The experiments were conducted using only three reactors (R2, R3, and R4 in Figure 3), with only the latter two reactors containing catalyst. The catalysts clearly promote the glycerol decomposition rate and higher conversion were measured compared to noncatalytic reforming. A typical figure with the gas concentration as a function of the tempera-

ture for a Ni based catalyst is given in Figure 8. The equilibrium curves were calculated using a model described in literature [18].

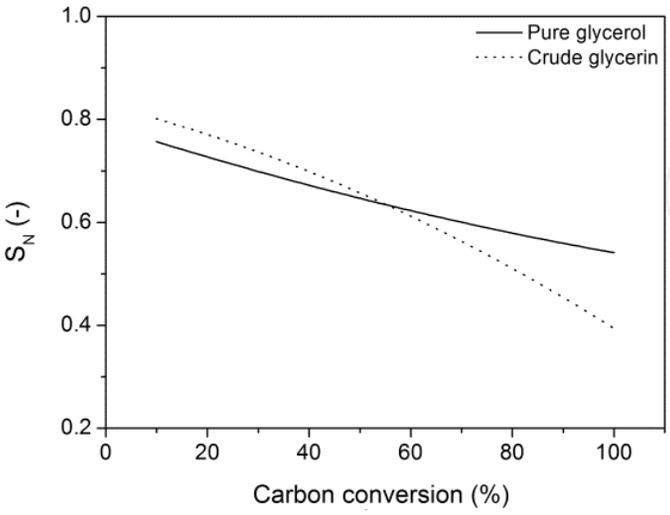

Figure 7. S_N for pure glycerol and crude glycerin as a function of the carbon conversion.

The gas composition is a function of the temperature and in this case equilibria are reached at temperatures exceeding 780 K. This catalyst strongly promotes methanation, as the CH_4 concentration is much higher than in noncatalytic reforming. At the higher temperatures the CH_4 concentration goes down according to thermodynamics. When a Ni based catalyst is used the WGS reaction (Eq. 11) is at equilibrium and almost all CO is converted into CO_2. After the reforming experiments traces of coke were visually observed at the catalyst surface and the reactor wall.

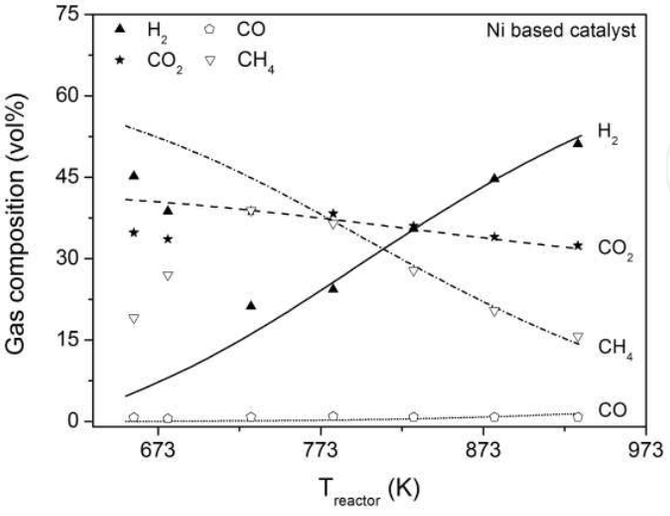

Figure 8. Gas concentration as a function of the temperature for a Ni based catalyst. P = 25.5 – 27.0 MPa, [glycerol] = 10 wt%. The curves represent equilibrium compositions, the symbols are experimental points [29].

The performance of this catalyst expressed in S_N, hydrocarbon content, and conversion is given in Figure 9. The conversion is almost complete over the whole temperature range. The concentration of hydrocarbons reaches a maximum as a function of the temperature and decreases at the higher temperatures. The S_N has the inverse profile and increases with higher temperatures, but still remains below 1.

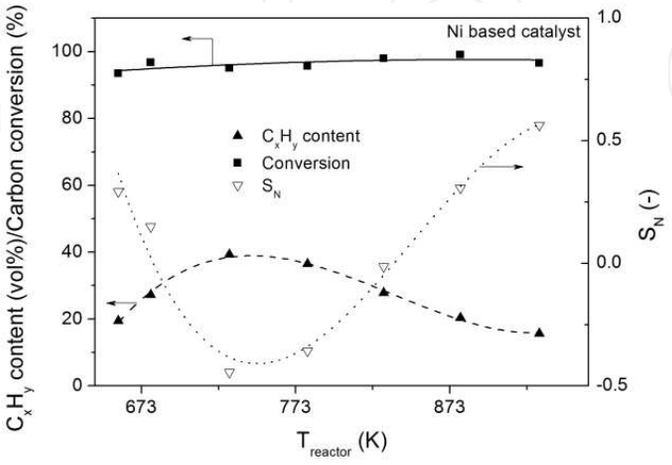

Figure 9. Performance indicators. P = 25.5 – 27.0 MPa, [glycerol] = 10 wt%, ϕ_{gly} = ± 100 g/h. The lines are trend lines and for illustrative purposes only.

3.4. Consequences of the reforming process for the integrated concept

The gas composition in noncatalytic reforming appeared to be not very attractive for methanol synthesis mainly due to the formation of hydrocarbons. Over a Ni based catalyst, CH_4 was the only hydrocarbon present in the gas phase. Its maximum concentration was close to 40 vol% at 730 K. A temperature increase resulted in a decreasing CH_4 concentration. A further decrease can be realized at higher temperatures and lower feed concentrations. Reduction of the hydrocarbon content has a positive effect on the S_N. At feed concentrations around 4 wt% and temperatures of approximately 1000 K, a S_N above 1 can be obtained. These conditions are the most attractive from a gas composition point of view (see also Section 5).

4. Methanol synthesis

4.1. Introduction to methanol synthesis

Methanol synthesis is conducted generally in catalytic gas-solid packed bed reactors. Three equilibrium reactions, taking place at the catalyst surface, are important: (i) the hydrogenation of CO (Eq. 17), (ii) the hydrogenation of CO_2 (Eq. 18), and (iii) the WGS reaction (Eq. 11):

$$CO + 2\,H_2 \leftrightarrow CH_3OH \tag{17}$$

$$CO_2 + 3\,H_2 \leftrightarrow CH_3OH + H_2O \tag{18}$$

All reactions are exothermic. The conversion of $CO+CO_2$ at chemical equilibrium is a function of pressure, temperature, and gas composition (see Figure 10).

Methanol synthesis at industrial scale was initiated by BASF in the 1920s. The operating temperatures were high (573 – 633 K) because of the low catalyst activity [30, 31]. High pressures (15 – 25 MPa) were needed to obtain reasonable conversions. When more active Cu based catalysts and better syngas purification techniques became available, the operating temperature and pressure could be reduced. This development led to the so-called low pressure methanol synthesis process (5 – 10 MPa, 490 – 570 K) which was developed by ICI in the 1960s. Since then, most high pressure units have been converted to low pressure systems [31, 32]. Both synthesis processes require large recycle streams of unconverted syngas due to the limited conversion per reactor pass as is shown in Figure 10 [32]. The reactor temperatures can be lowered further (to 463 – 520 K) due to the recent development of more active catalysts.

In the research study described in this chapter, a combination of low temperatures (468 – 545 K) and high pressures (15 – 25 MPa) is investigated. At this combination of pressure and temperature the Equilibria conversions towards methanol are high (see Figure 10).

4.2. Methanol condensation

The methanol conversion in conventional methanol synthesis is restricted by the chemical equilibrium as shown in Figure 10. There are several opportunities to circumvent the limitations imposed by thermodynamic equilibria and they mainly involve *in situ* removal of methanol. This can be done, for example, by methanol adsorption on fine alumina powder or dissolving methanol in tetraethylene glycol, n-butanol, or n-hexane [33-35]. Another method involves *in situ* condensation at a cooler inside the reactor [36]. With all the different methods mentioned higher syngas conversions were obtained but at the same time all methods have drawbacks including the use of other chemicals, complicated operation procedures, or low yields. Conversions beyond the chemical equilibrium can be obtained with *in situ* condensation of methanol and water without adsorbents or coolers. Condensation occurs at a combination of high operating pressures and low temperatures. Condensation has only been shown indirectly in literature by experimental observations of conversions beyond equilibrium or theoretical models [37-40]. We've demonstrated *in situ* methanol condensation visually in a view cell reactor. In this reactor a propeller-shaped stirrer was equipped with catalyst pellets. The view cell was operated semi-batch wise. Methanol synthesis started when syngas ($H_2/CO/CO_2$ = 70/28/2 vol%) was fed to the reactor. The most striking observation was *in situ* condensation at 20.0 MPa and 473 K (Figure 11). Liquid formation was also observed at 17.5 MPa and 473 K and for other gas compositions [41].

http://dx.doi.org/10.5772/53691

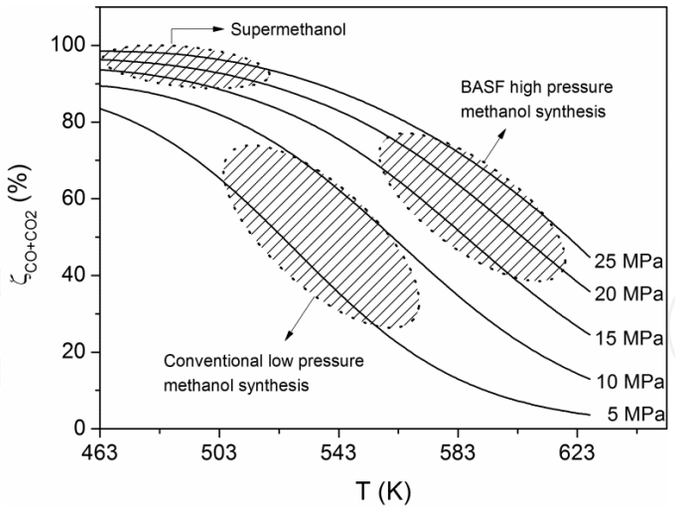

Figure 10. Equilibria in methanol synthesis. Approximate conditions are given for (i) conventional processes, (ii) BASF's high pressure process, and (iii) Supermethanol (this work). Syngas: $H_2/CO/CO_2/CH_4$ = 67/24/4/5 vol% [8].

The liquid accumulated in the view cell upon prolonged reaction times. Part of the catalyst became immersed and even after complete immersion methanol synthesis from syngas bubbling through the liquid went on.

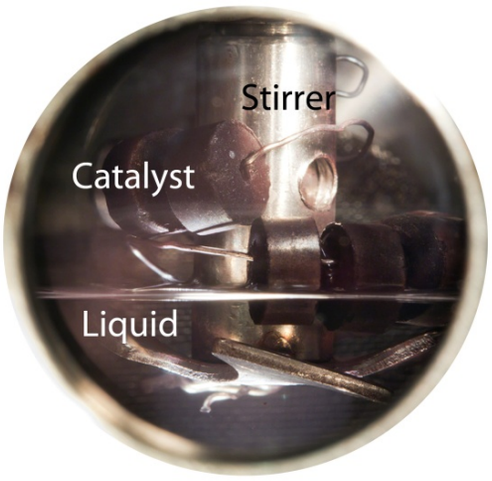

Figure 11. Liquid formation in a view cell. P = 20.0 MPa, T = 473 K, Syngas: $H_2/CO/CO_2$ = 70/28/2 vol%.

The liquid phase consists of mainly methanol and water. The exact composition is a function of conversion, process conditions, and syngas composition. Condensation may have positive effects on methanol synthesis as will be demonstrated later on in this chapter. Conversions higher than the chemical equilibrium are achieved and almost complete conversion of the limiting component(s) can be obtained at appropriate conditions. As a consequence, recycle and purge streams are not necessary, the limitations on the S_N become less strict, and methanol yields may be increased for a given reactor volume. Most probably the reaction rates in methanol synthesis will be higher at high pressure than at conventional conditions due to

higher partial pressures of the reactants, however, experimental validation is required to validate this hypothesis.

4.3. Modelling simultaneous phase and chemical equilibria

A solution model to calculate equilibrium conversions in methanol synthesis including condensation was developed. The effects of process conditions (pressure, temperature, gas composition) can be assessed with the model. Dew points were calculated using Eq. 19 for a given pressure and temperature for each component [42, 43]. A modification of the Soave-Redlich-Kwong equation of state (for polar components) was used to calculate the fugacities of each phase.

$$f_i^V = f_i^L \tag{19}$$

Where, f_i is the fugacity of component i, V and L denote the vapor and the liquid phase respectively. The simultaneous chemical and phase equilibria were calculated using Eq. 19 and theoretical equilibrium constants [44]. The model is described and explained in more detail in the literature [45].

A typical equilibrium diagram for $H_2/CO/CO_2/CH_4$ = 70/5/20/5 vol% is given in Figure 12. The equilibrium diagram for this gas composition illustrates clearly the influence of condensation on the equilibrium conversion.

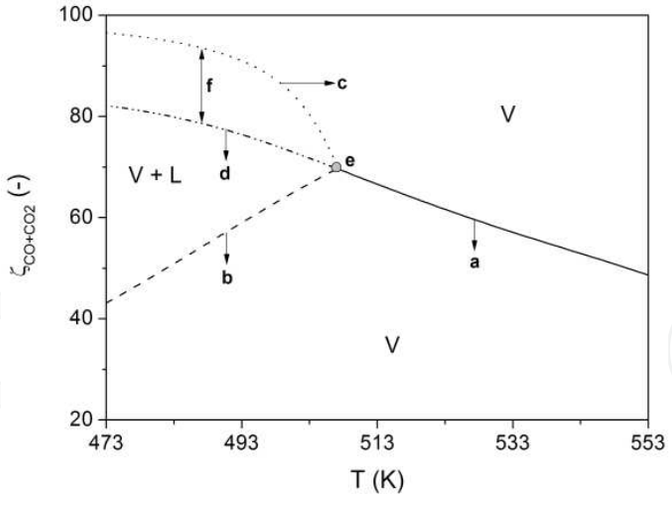

Figure 12. Example of an equilibrium conversion diagram including chemical and phase equilibria. Gas phase equilibrium curve (**a**), dew point curve (**b**), equilibrium curve including liquid formation (**c**), extrapolation of the gas phase equilibrium curve (**d**), point where all equilibrium curves merge (**e**), difference between extrapolated gas phase equilibrium and equilibrium including liquid formation (**f**). *P* = 20.3 MPa, syngas: $H_2/CO/CO_2/CH_4$ = 70/5/20/5 vol% [41].

In the diagram, 4 curves are shown. Curve **a** (solid curve) is the gas phase equilibrium curve. Curve **b (**dashed curve) is the conversion at which a dew point occurs. Curve **c (**dotted curve) is the equilibrium curve including condensation and curve **d** (dashed-dotted

curve) is an extrapolation of the gas phase equilibrium curve. The 4 curves come together in point **e.** In this point (T = 507 K), the gas composition is at equilibrium and the dew point temperature of the mixture equals the reactor temperature. Curve **d**, the extrapolation of curve **a,** is the equilibrium conversion when condensation is neglected. When condensation occurs, the equilibrium conversion is much higher which is indicated by the arrow marked **f** (difference between curve **c** and **d)** in Figure 12. The value for **f** amounts to 13.9% at 473 K (ζ_{CO+CO2} = 82.6% vs. ζ_{CO+CO2} = 96.5%) for this particular gas composition.

4.4. High pressure methanol synthesis in a packed bed reactor

Methanol synthesis experiments were conducted in the packed bed reactor using 3 different syngases (see Table 1) and pressures of about 20 MPa. Gas 1 and 2 represent typical methanol synthesis gases (S_N = 2.0 – 2.3), with gas 1 rich in CO and gas 2 rich in CO_2. The composition of gas 3 resembles a typical syngas obtained in the reforming of glycerol or biomass in general. For this gas S_N < 2 and H_2 is the limiting component. The experiments were performed with a large amount of catalyst to approach the equilibrium conversion.

To check the assumption of equilibrium at the reactor outlet and that the experiments were not conducted in the kinetic regime experiments with different flow rates were conducted for gas 1. For the experiments, methanation and the formation of higher hydrocarbons were negligible. For gas 1, the CO+CO_2 conversion at 468 K and 20.7 MPa was 99.5%, which is 7.7% higher than the equilibrium conversion calculated at 7.5 MPa. For gas 2, the difference between methanol synthesis at 20 and 7.5 MPa is more pronounced. The CO+CO_2 conversion at 484 K was 92.5% which is 46.9% higher than the equilibrium conversion predicted at 7.5 MPa.

Gas	H_2	CO	CO_2	CH_4	C_2H_6	S_N	Remarks
	(vol%)	(vol%)	(vol%)	(vol%)	(vol%)	(-)	
1	67.0	24.4	3.5	5.1	-	2.3	Industrial gas
2	69.9	5.0	20.0	5.1	-	2.0	CO_2 rich gas
3	54.2	28.9	10.9	4.0	2.0	1.1	Simulated RSCW gas

Table 1. Compositions of the different gases used in methanol synthesis.

The experimental and predicted equilibrium conversions for gas 1 and gas 2 are shown in Figure 13. At temperatures above 495 K for gas 1 and 507 K for gas 2 only a gas phase is present, while at lower temperatures condensation occurs. Methanol production continues in the two phase system until phase equilibrium and chemical equilibrium are reached. At the lowest temperatures in the range, the CO+CO_2 conversion is nearly complete for gas 1 (Figure 13A). The conversion of CO+CO_2 decreased with increasing temperature as dictated by thermodynamics. The experimental conversions coincide nicely with the conversion predicted by the model. The effect of condensation was more pronounced for gas 2 (Figure

13B). Here, the experimental conversion is even 12.7% higher than the extrapolated gas phase equilibrium curve (ζ = 79.8% vs. 92.5% at 484 K).

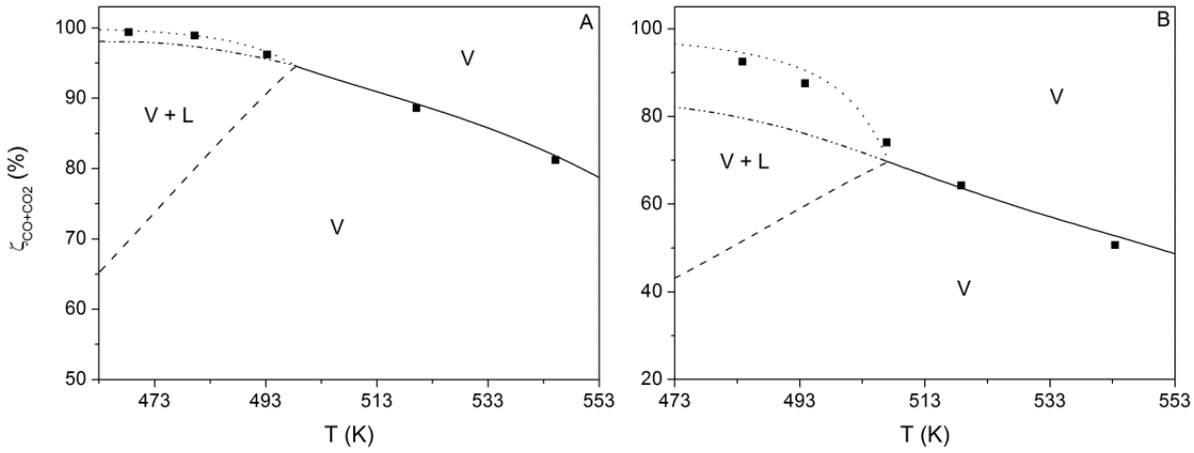

Figure 13. Equilibrium diagrams for methanol synthesis. Gas 1 (A), *P* = 19.7 MPa [41]. Gas 2 (B) [45], *P* = 20.3 MPa. Symbols: experimental data; curves: model results.

In Figure 14, both the $CO+CO_2$ conversion (Figure 14A) and the H_2 conversion (Figure 14B) are depicted for gas 3. At the two lower temperatures, the equilibrium predictions coincide nicely with the experimental data for, but this changes at the higher temperatures most probably due to the formation of HA. This is a common phenomenon for systems at higher temperatures with high CO partial pressures [46, 47]. HA formation is not included in the equilibrium model and this explains the deviations at higher temperatures.

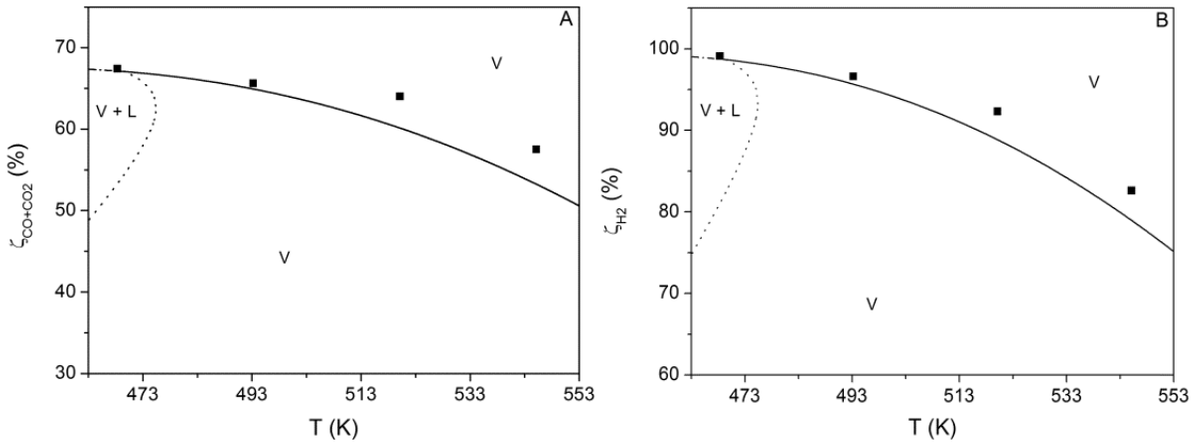

Figure 14. Equilibrium diagram for methanol synthesis from gas 3 including the dew point curve for ζ_{CO+CO2} (A) and ζ_{H2} (B). Symbols: experimental data; curves: model results. *P* = 19.4 MPa [45].

The concentration of the main HA is given in Figure 15. The methanol concentration clearly decreases over the temperature range in favor of the HA. Based on thermodynamics the formation of higher alcohols is expected as HA formation is favored over methanol [48]. The

main HA formed in the experiments were ethanol and 1-propanol followed by 1-butanol, 2-methyl-1-propanol, and 2-methyl-1-butanol.

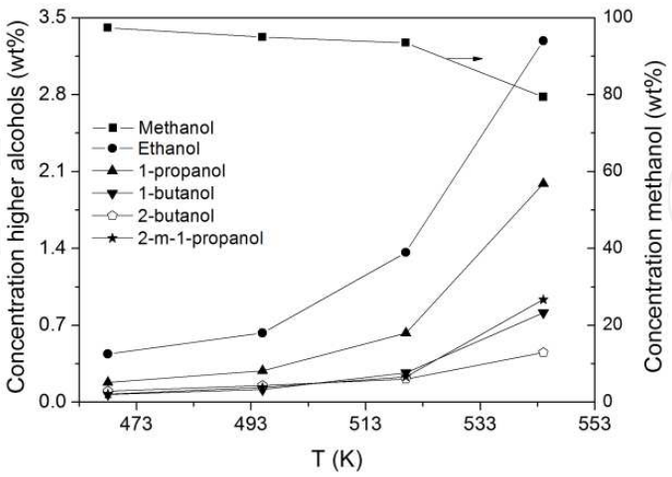

Figure 15. Methanol and HA concentrations as a function of the temperature for gas 3. P = 19.9 MPa.

4.5. Consequences of methanol synthesis for the integrated concept

The main result from high pressure methanol synthesis experiments is the observation that high conversions of the limiting component are attainable. These conversions are higher than calculated on the basis of chemical gas phase equilibria and are due to condensation. When the HA concentration was low, the experimental conversion corresponded nicely with the equilibria predicted. In conclusion, when a combination of high pressure and moderate temperature ($463 \leq T \leq 500$ K) is used, high conversions for glycerol derived syngases are expected.

5. Demonstration of the integrated concept

To demonstrate the integrated concept for methanol synthesis, experiments were conducted in the integrated continuous unit depicted in Figure 3 [8]. Both, process conditions and recycle options of the reforming section were investigated to maximize methanol yields. This requires proper operating conditions for each reactor section (reforming, methanol synthesis) to limit by-product formation (e.g. CH_4, higher hydrocarbons, and HA) and to allow operation at high equilibrium conversions in methanol synthesis. In this section, both the results for the overall integrated process will be discussed as well as the result for the reformer section in these experiments. Four different cases are considered with different feed concentrations and operating conditions. An overview of the experiments is presented in Table 2 and a short resume is given below.

The first case is considered the base case. The experiment of the base case was conducted using the LPS without recycling the effluent water (see Figure 3). Part of the gas produced is

lost as it dissolves in the aqueous phase that leaves the process. In case 2, 3, and 4 the effluent water from the reformer is recycled after the HPS. Operating with a recycle stream at high pressure in RSCW is a unique feature. As a consequence of the recycle stream no gas is lost in the reformer section through the LPS and additionally, the water consumption of the process is reduced significantly. In these experiments the glycerol reforming is carried out catalytically by using the Ni based catalyst in combination with higher temperatures. All C_{2+} hydrocarbons are then reformed and the CH_4 equilibrium concentration decreases (with higher temperatures) yielding a more attractive gas composition [29].

Finally, in case 4 an extra methanol synthesis packed bed (P1) was added to achieve equilibrium gas phase conditions at the outlet. The methanol synthesis section now consists of 3 packed bed reactors (P1 – P3) in series. The three packed beds were operated at different temperatures, viz. ± 518 K (P1), ± 503 K (P2), and 481 – 482 K (P3) by cooling the heating medium between the reactors. The reaction rate in methanol synthesis depends strongly on temperature. Higher temperatures lead to higher reaction rates. In the first reactor (P1) the reaction rate will be relatively high while the second (P2) and third (P3) are used to achieve equilibrium. Typical run times for the experiments were 6 – 10 h and steady state was reached in approximately 2 h. In case 4 the operating time exceeded 20 h of which 16 h in the integrated mode. This experiment is considered as the long duration experiment.

Case	Catalyst[a] (g)			Recycle	Catalyst[b] (g)		
	R3[d]	R4[d]	R5[d]		P1[d]	P2[d]	P3[d]
1	-	-	-		-	50	51
2	10	10	3	yes	-	50	51
3	10	10	3	yes	-	50	51
4[c]	10	10	3	yes	51	50	51

[a]Ni based catalyst.

[b]A commercial $Cu/ZnO/Al_2O_3$ catalyst.

[c]The catalyst in the reforming section was replaced by fresh catalyst.

[d]R = reformer, P = packed bed reactor for methanol synthesis.

Table 2. Overview of experiments in the integrated unit. R3-5 and P1-3 correspond with the reactors in Figure 3 [8].

5.1. Reformer performance

Typical conditions for the reformer section (see Figure 3) for these experiments were pressures from 24 to 27 MPa and temperatures between 948 and 998 K. At these conditions the residence times of the reformer section (R1 – R5) were in the range of 30 – 35 s. The composition and quantity of the off-gas were analyzed to determine the carbon balance. The hydrocarbon concentration in the off-gas is the summation of the concentrations of CH_4 and C_2H_6. The main results of the glycerol reformer section are summarized in Table 3.

Carbon balance closure for the reformer is very satisfactorily and was between 95 and 104%. The glycerol conversion was almost complete for all experiments, which is in line with previous work [18, 29]. The syngas produced had the following composition range: $H_2/CO/CO_2/C_xH_y$ = 44 – 67/1 – 21/16 – 34/2 – 18 vol%, $0.7 \leq S_N \leq 1.2$. The results for each case will be discussed separately in the following section.

5.1.1. Base case

The base case experiment was conducted with a glycerol feed concentration of 10 wt% at 27 MPa and 948 K. The unit was operated without a catalyst in the reformer section and in a once-through mode. Part of the gas (ca. 13%) dissolved in the effluent stream from the LPS (see Figure 3, D_2) and is not used for the subsequent methanol synthesis. Due to the absence of catalysts, a significant amount of CO is present in the syngas. The product gas has a relatively low S_N value of 0.7, which is mainly caused by the formation of hydrocarbons (18 vol % consisting for approximately ⅔ of CH_4 and ⅓ of C_2H_6).

Case	P_a	T_{R5}	ϕ_{gly}	[Gly.]	H_2	CO	CO_2	C_xH_y	S_N	ζ_{gly}	C_{bal}
	(MPa)	(K)	(g/h)	(wt%)	(vol%)				(-)	(%)	(%)
1	27	948	106	10.4	44	21	17	18	0.7	96[b]	96
2	24	998	97	± 10	55	2	32	11	0.7	99.9[c]	97
3	24	998	35	± 4	59	1	34	6	0.8	99.9[c]	104
4	26	998	35	± 4	66	1	30	3	1.2	99.9[c]	95
Loc.[d]	A_{1-3}	B	C		D_1	D_1	D_1	D_1			

[a]The pressure is an average pressure. The actual operating pressure is the indicated pressure ± 1 MPa.

[b]Based on carbon content in the effluent water.

[c]Experiment conducted in recycle mode. Glycerol conversion is estimated based on previous work [29].

[d]Locations where the parameters were measured (see Figure 3).

Table 3. Results of the reforming section (before methanol synthesis) [8].

5.1.2. Case 2 – 4

The intention for case 2 was to aim for higher S_N values. A Ni based catalyst was added to reactor R4 and R5 to reform the higher hydrocarbons. As a consequence the WGS reaction also reached equilibrium and almost all CO was converted into CO_2 [29]. The temperature of reactor R5 was increased with 50 K compared to the base case to aim for a more advantageous equilibrium composition (less CH_4). Furthermore, the effluent water was recycled at high pressure. Recycling the effluent water drastically reduces the water consumption of the process. The recycle flow was adjusted in such a way that the aqueous reactor inlet flow was comparable to the inlet flow in the base case. Compared to the base case no gas was lost through the effluent stream from the LPS. The gas composition obtained over this catalyst differed substantially from the

base case. The CO concentration was reduced from 21 vol% to 1 – 2 vol% and the concentration of the hydrocarbons was significantly lower and approached equilibrium ($C_2H_6 \approx 0$ vol% and $CH_4 \approx 11$ vol%). The S_N value was similar to the base case.

For case 3 the glycerol feed concentration was reduced to approximately 4 wt%. The H_2 and CO_2 concentration increased compared to the base case, whereas the CO and hydrocarbon concentration were lower, resulting in a slightly more attractive S_N value of 0.8. In the last case (4), a fresh reforming catalyst was used leading to the lowest hydrocarbon concentration and the highest H_2 concentration of all experiments. For instance, C_2H_6, which accounted for ⅓ of the hydrocarbon content in the base case, was not detected in the product gas. The S_N increased to 1.2 which is close to the theoretical maximum of 1.33 (Eq. 3).

5.2. Performance of the integrated process

The results for the integrated process, including methanol synthesis, are presented in Table 4. The equilibria in methanol synthesis were calculated with the data from Table 3 as input and the equilibrium model described in Section 4.3. If applicable, condensation of methanol and water was accounted for in the equilibrium calculations [45]. The equilibrium data should be considered with some care, because the results are based on the assumption of constant gas composition and gas flow from the reformer section. As for the reforming experiments, all methanol synthesis experiments have good closures of the carbon balance (93 – 96%), particularly when regarding the complexity of the integrated process. A detailed summary of the experimental results of the integrated process is given below. As in section 5.1, case 1 is considered as base case and the results of the other experiments are compared to this experiment.

Case	T	H_2	CO	CO_2	C_xH_y	η^a	MeOH[b]	H_2O	ζ_{CO+CO2}	ζ_C	C_{bal}
	(K)			(vol%)				(wt%)		(%)	
1	468	3	2	44	51	0.27	99	1	58	26	95
equi	468	5	2	44	49	0.28	99	1	59	28	-
2	498	42	0	40	18	0.29	67	33	35	27	96
equi	498	25	1	46	28	0.35	66	34	45	33	-
3	483	49	0	40	11	0.27	65	35	39	26	93
equi	483	15	1	61	23	0.50	65	35	54	48	-
4	481	20	0	60	20	0.62	65	35	71	60	94
equi	481	11	1	69	19	0.65	65	35	70	62	-
Loc.[c]	**E**	**G**	**G**	**G**	**G**	**F**	-	-	-	-	-

[a]Units = (kg methanol/kg glycerol).

[b]The liquid phase is assumed to consist of water and methanol. The methanol concentration here is calculated by 100 wt% – (water concentration). The exact composition of the organic phase is given in Table 5.

[c]Locations where the parameters were measured (see Figure 3).

Table 4. Results of methanol synthesis from glycerol derived syngas [8].

5.2.1. Base case

In the experiment in case 1, the methanol synthesis reactors were operated at 468 K. Hydrocarbons are inert in methanol synthesis and as a results their concentration increased strongly in the off-gas of the methanol synthesis reactor to over 50 vol%. The H_2 and CO concentration in the outlet of the methanol reactor were 3 and 2 vol%, respectively. The CO_2 concentration increased compared to the reforming gas, as mainly CO was converted to methanol. The gas composition and liquid yield at the exit of the methanol reactor were close to equilibrium, with the liquid yield slightly lower and experimental conversion slightly higher than predicted by equilibrium modelling. The overall carbon conversion was 26% which is equal to a methanol yield of 0.27 kg methanol/kg glycerol. The conversion of 26% is the highest conversion possible with such a syngas composition, because equilibrium was reached.

5.2.2. Case 2 – 3

In case 2, a different approach was followed. Due to the Ni based catalyst in the reforming section the hydrocarbon concentration decreased and almost all C_2H_6 was reformed. Furthermore, almost all CO was converted into CO_2, which therefore became the main carbon source of methanol. The temperature of the methanol synthesis reactors was increased compared to the base case (from 468 – 498 K), because methanol synthesis from mainly CO_2 proved to be slower than methanol synthesis from CO. The methanol yield was, with 0.29 kg methanol/kg glycerol, similar to the base case, but in case 2 equilibrium was not reached. Higher conversion are thus possible with longer residence times.

For case 3 the glycerol feed flow was reduced with a factor 3 to improve the gas composition, resulting in a reduction in feed gas flow. Therefore, to obtain higher conversion, the temperature of the methanol synthesis reactor was reduced to 483 K. Again, the carbon conversion and methanol yield (0.27 kg methanol/kg glycerol) were comparable to the base case, but remained far from equilibrium.

5.2.3. Case 4: Long duration experiment in the integrated unit

In case 4 (long duration run, 20 h) an extra methanol synthesis packed bed (P1) was filled with catalyst. The methanol synthesis reactors were operated at three different temperatures (± 518 K (P1), ± 503 K (P2), and 481 – 482 K (P3). The lowest hydrocarbon concentration in the gas phase after the reformer was observed due to the use of a fresh reforming catalyst. As a consequence the corresponding carbon conversion in the methanol synthesis unit increased to 60% (η = 0.62 kg methanol/kg glycerol). Nevertheless, even higher methanol yields are possible as equilibria were not yet achieved. In the first 4 h of the long duration experiment, only the reformer section was operated. Methanol synthesis was carried out over a 16 h period and the hourly liquid methanol yields and volumetric flows at the exit of the methanol synthesis unit (point G in Figure 3) are shown in Figure 16.

Though some scattering in the methanol yield can be noted (due to some pressure fluctuation and uncontrolled release by the back pressure valve during the experiment), the integrated system was running steadily and the methanol yield was more or less constant. The

selectivity (σ) is depicted in Figure 16B. The methanol selectivity is equal to the carbon conversion and amounts to 60% on average. An average value of 8.7% of the carbon present in glycerol ends up as CH_4. The scattering pattern for the methanol selectivity is similar to the scattering in the methanol yield in Figure 16A. The selectivity towards CH_4 is also more or less constant. It seems that no deactivation or reduced activity for both the reformer section and the methanol synthesis section were observed during the course of the experiment.

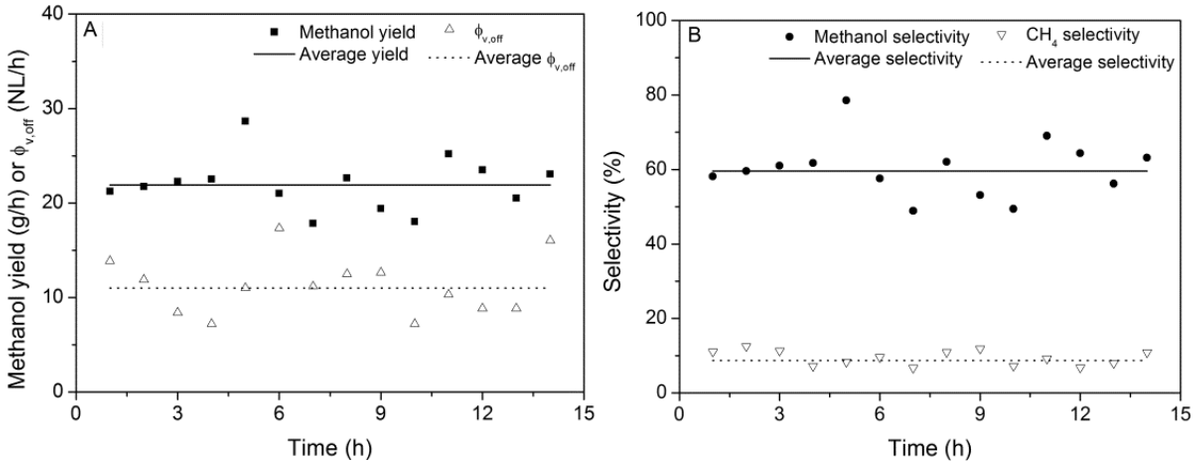

Figure 16. Methanol yields from glycerol and volumetric flow at the exit of the methanol reactor of the long duration experiment (A). Carbon selectivity towards methanol and CH_4 (B) [8].

5.3. Liquid composition after methanol synthesis reactor

The main constituents of the liquid products of the integrated experiments are given in Table 5. The liquid phase was analyzed on methanol, water, and the eight most common HA. In general, the concentration of HA was very low (< 0.23 wt% of the total and < 0.24 wt% of the organic fraction), probably due to the low temperatures of the methanol synthesis and the high CO_2 content of the feed gas, leading to the formation of water [46]. Ethanol was the most predominant among the HA, with a maximum concentration of 1.2 wt‰. Noticeably, when methanol was predominantly synthesized from CO_2 (case 2 – 4) the concentrations of HA were negligible. This is in agreement with literature data which show that the concentrations of HA decrease at higher H_2/CO ratios in the syngas feed [46, 47].

Case	Liquid product				Higher alcohols				
	MeOH	H_2O	HA	Purity[a]	EtOH	2-propanol	1-butanol	2-m-1-propanol	2-m-1-butanol
	(wt%)				(wt‰)				
1	97.8	1.1	0.23	99.8	1.2	0.7	0.2	0.2	0.1
2	66.5	33.0	0.00	99.9	0.0	0.0	0.0	0.0	0.0
3	65.9	34.6	0.00	99.9	0.0	0.0	0.0	0.0	0.0
4	65.1	34.9	0.01	99.9	0.1	0.0	0.0	0.0	0.0

[a]Methanol content of the organic fraction.

Table 5. Composition of the liquid phase [8].

5.4. Process analysis

The experiments conducted in the integrated unit were aimed at obtaining high carbon conversions and methanol yields when reforming aqueous glycerol solutions to syngas followed by methanol synthesis. The gas composition after reforming appeared to be the most critical factor and has a major effect on the final methanol yield. Particularly the formation of hydrocarbons should be avoided in the reformer section as hydrocarbons are inert in the subsequent methanol synthesis. Therefore, hydrocarbon reduction was the main objective in the experimental reformer program and was pursued by the application of catalysts, higher reforming temperature, and reduction of the feed concentration. Application of a suitable catalyst (Ni based) indeed led to a considerable reduction in the amount of hydrocarbons in the reformer off-gas, though as a consequence almost all CO was converted into CO_2. Further research will be required to identify reformer catalysts that promote glycerol decomposition rates and hydrocarbon reforming, but do not enhance the WGS reaction. In this respect, Ir-based catalysts are promising because of good performance in aqueous phase reforming [49].

The conversion of CO into CO_2 in the reformer section, as observed when using the Ni based catalyst, is not detrimental for the subsequent methanol synthesis. With the commercial methanol synthesis catalyst used in this study, CO_2 hydrogenation is possible, as was also proven here, though the overall reaction rates in methanol synthesis are lower than in case of CO hydrogenation [50]. An advantage, however, of CO_2 hydrogenation is the high purity of the organic fraction, as the formation of HA is suppressed by, most probably, the presence of water [46, 51].

In the demonstration of the integrated concept, pure glycerol was used as feedstock for the process. When crude glycerin is used salts are present and they have to be removed upfront. Continuous salt removal is possible and has been demonstrated in the literature [52].

6. Conclusion

A successful experimental demonstration of glycerol conversion to methanol was shown by the integration of two processes. Glycerol was reformed in supercritical water to syngas and the syngas was subsequently converted to methanol. Before integration of the two processes the processes were investigated individually. In glycerol reforming a gas containing mainly H_2, CO, CO_2, CH_4, and C_2H_6 was produced. When a Ni based catalyst was used the higher hydrocarbons were reformed and CH_4 approached its equilibrium concentration. In methanol synthesis *in situ* condensation was observed which positively influences the equilibrium conversion. At temperatures around 473 K and pressures above 20 MPa almost complete conversion of the limiting components was obtained.

The methanol yields of the integrated process depended mainly on the gas composition obtained in the glycerol reforming process, which appeared to be the most attractive for methanol synthesis at high temperature and low feed concentration in combination with a Ni based catalyst. The continuous unit was modified during the experimental program to increase the methanol yields. The effluent water of the reformer section was recycled at high pressure, to reduce the water consumption of the process. The highest methanol yield of 0.62 kg methanol/kg glycerol was obtained using the Ni based catalyst in the reformer section and recycling of the effluent water. In this particular experiment glycerol was converted to mainly H_2 and CO_2 and smaller amounts of CH_4 and CO. In this experiment, 60% of the carbon present in the glycerol ends up in methanol. These yields are close to the equilibrium yields. The integrated unit was operated smoothly for more than 16 h without catalyst deactivation.

The scope of the project is much broader than the production of methanol from glycerol for the reuse in biodiesel production. Due to the investigation of the individual processes more insights in reforming and methanol synthesis were obtained. Furthermore, the feedstock for the reforming process was glycerol in this case, but several types of biomass (preferably liquid) including aqueous phase fractions from pyrolysis oil upgrading, black liquor, etc. can be used for the reforming process. When these types of feedstocks are 'green' renewable methanol can be produced, which is a promising process for the (near) future.

Acknowledgements

The authors acknowledge the assistance given by the following companies and publishers in permitting the reproduction of figures, tables, and portions of the text (with minor adaptations) from their publications.

Figure 1 was published with courtesy of Desmet Ballestra [16]. The data has been obtained from the European Biodiesel Board.

Figures 3, 10, and 16 and Tables 2 – 5, and large portions of Sections 1, 2, and 5 were originally published in Chemical Engineering Journal [8] and used with permission.

Figure 4 [19] is reproduced in modified form by permission of The Royal Society of Chemistry (http://dx.doi.org/10.1039/B810100K).

Figures 5 and 8 and portions of Section 3 were originally published in the Journal of Supercritical Fluids [29] and used with permission.

Figure 6 and portions of Section 3 were originally published in the Journal of Supercritical Fluids [18] and used with permission.

Figures 12 and 13B and portions of Section 4 were originally published in Chemical Engineering Science [41] and used with permission.

Figures 13A and 14 were reprinted with permission from [45], copyright 2012 American Chemical Society.

The authors would like to acknowledge the EU for funding the work through the 5th and the 7th Framework Program (Superhydrogen: ENK5-2001-00555 and Supermethanol: no. 212180) and Agentschap NL (EOSLT05020). The initial screening for Supermethanol was funded by Agentschap NL (no. 0268-05-04-02-011 and no. NEOT01008). We also would like to thank the partners of the Supermethanol project, and in particular D. Assink, K.P.J. Lemmens, S.D.G.B. Nieland from BTG, The Netherlands for building and operating the units, J. Vos from BTG for proofreading, and E. Wilbers, J.G.M. Winkelman and J. Bos from the University of Groningen, The Netherlands for their assistance in the work concerning the methanol synthesis and J. Bos for taking the pictures of the reactor. V.A. Kirillov from the Boreskov Institute of Catalysis, Russia is acknowledged for supplying the reforming catalyst.

Author details

Joost G. van Bennekom[1], Robertus H. Venderbosch[2] and Hero J. Heeres[1*]

*Address all correspondence to: h.j.heeres@rug.nl

1 University of Groningen, Green Chemical Reaction Engineering, Groningen, The Netherlands

2 BTG, Biomass Technology Group, Enschede, The Netherlands

References

[1] Olah GA, Goeppert A, Prakash GKS. Beyond oil and gas: The methanol economy. Weinheim: Wiley-VCH; 2006.

[2] Beenackers AACM, Swaaij WPM van. Methanol from wood II. Current research and development programs. Int. J. Sol. Energy. 1984; 2(6) 487-519.

[3] Beenackers AACM, Swaaij WPM van. Methanol from wood I. Process principles and technologies for producing methanol from biomass. Int. J. Sol. Energy. 1984; 2(5) 349-367.

[4] Xiuli Y. Synthesizing methanol from biomass-derived syngas. Hong Kong: The university of Hong Kong; 2005.

[5] Norbeck JM, Johnson K. Evaluation of a process to convert biomass to methanol fuel. In: Agency, U. S. E. P., editor. Cincinnati2000.

[6] Ekbom T, Lindblom M, Berglin N, Ahlvik P. Cost-competitive, efficient biomethanol production from biomass via black liquor gasification (Nykomb Synergetics AB, 2003).

[7] Knoef HAM. editor Handbook Biomass Gasification. Enschede: BTG Biomass Technology Group; 2005.

[8] Bennekom JG van, Venderbosch RHV, Assink D, Lemmens KPJ, Heeres HJ. Bench scale demonstration of the Supermethanol concept: The synthesis of methanol from glycerol derived syngas. Chem. Eng. J. 2012; 207-208 245-253

[9] Borgwardt RH. Methanol production from biomass and natural gas as transporation fuel. Ind. Eng. Chem. Res. 1998; 37 3760-3767.

[10] Chmielniak T, Sciazko M. Co-gasification of biomass and coal for methanol synthesis. Appl. Energy. 2002; 74 393-403.

[11] Hamelinck CN, Faaij APC. Future prospects for production of methanol and hydrogen from biomass. J. Power Sources. 2002; 111 1-22.

[12] Li H, Hong H, Jin H, Cai R. Analysis of a feasible polygeneration system for power and methanol production taking natural gas and biomass as materials. Appl. Energy. 2010; 87 2846-2853.

[13] Rens GLMA van, Huisman GH, Lathouder H de, Cornelissen RL. Performance and exergy analysis of biomass-to-fuel plants producing methanol, dimethylether or hydrogen. Biomass Bioenergy. 2011; 35 S145-S154.

[14] Xu Y, Ye TQ, Qiu SB, Ning S, Gong FY, Liu Y, Li QX. High efficient conversion of CO_2-rich bio-syngas to CO-rich bio-syngas using biomass char: A useful approach for production of bio-methanol from bio-oil. Bioresour. Technol. 2011; 102 6239-3245.

[15] Directive 2009/28/EC of the European Parliament and of the Council of 23 April 2009 on the promotion of the use of energy from renewable sources and amending and subsequently repealing Directives 2001/77/EC and 2003/30/EC. Official Journal of the European Union. Strasbourg 2009. p. 47.

[16] Greyt W de. Introduction on glycerol as co-product from biodiesel plants. Innovative uses of glycerol from the biodiesel process; 2011; Brussels.

[17] Bennekom JG van, Vos J, Venderbosch RH, Torres MAP, Kirilov VA, Heeres HJ, Knez Z, Bork M, Penninger JML. Supermethanol: Reforming of crude glycerine in su-

percritical water to produce methanol for re-use in biodiesel plants. 17th European Biomass Conference and Exhibition; 2009; Hamburg.

[18] Bennekom JG van, Venderbosch RH, Assink D, Heeres HJ. Reforming of methanol and glycerol in supercritical water. J. Supercrit. Fluids. 2011; 58(1) 99-113.

[19] Peterson AA, Vogel F, Lachance RP, Fröling M, Jr. MJA, Tester JW. Thermochemical biofuel production in hydrothermal media: A review of sub- and supercritical water technologies. Energy Environ. Sci. 2008; 1 32-65. http://dx.doi.org/10.1039/B810100K

[20] Toor SS, Rosendahl L, Rudolf A. Hydrothermal liquefaction of biomass: A review of subcritical water technologies. Energy. 2011; 36 2328-2342.

[21] Gadhe JB, Gupta RB. Hydrogen production by methanol reforming in supercritical water: suppression of methane formation. Industrial and Engineering Chemistry Research. 2005; 44(13) 4577-4584.

[22] Brunner G. Near critical and supercritical water. Part I. Hydrolytic and hydrothermal processes. J. Supercrit. Fluids. 2009; 47 373-381.

[23] Elliot DC. Catalytic hydrothermal gasification of biomass. Biofuels, Bioprod. Biorefin. 2008; 2 254-265.

[24] Kruse A. Supercritical water gasification. Biofuels, Bioprod. Biorefin. 2008; 2 415-437.

[25] Kruse A. Hydrothermal biomass gasification. J. Supercrit. Fluids. 2009; 47 391-399.

[26] Matsumura Y, Minowa T, Potic B, Kersten SRA, Prins W, Swaaij WPMv, Beld Bvd, Elliot DC, Neuenschwander GG, Kruse A, Jr. MJA. Biomass gasification in near- and supercritical water: Status and prospects. Biomass Bioenergy. 2005; 29 269-292.

[27] Basu P, Mettanant V. Biomass gasification in supercritical water - A review. Int. J. Chem. Reactor Eng. 2009; 7 1-61.

[28] Weingärtner H, Franck EU. Supercritical water as a solvent. Angew. Chem. Int. Ed. 2005; 44 2672-2692.

[29] Bennekom JG van, Kirillov VA, Amosov YI, Krieger T, Venderbosch RH, Assink D, Lemmens KPJ, Heeres HJ. Explorative catalyst screening studies on reforming of glycerol in supercritical water. J. Supercrit. Fluids. 2012; 70 171-181.

[30] Mittasch A, Winkler K, Pier M. Verfahren zur Gewinnung organischer Verbindungen durch katalytische Gasreaktionen. DE441433, Germany, 1923.

[31] Skrzypek J, Stoczynski J, Ledakowicz S. Methanol synthesis. Warsaw: Polish Scientific Publishers PWN; 1994.

[32] Supp E. How to produce methanol from coal. Berlin: Springer-Verlag; 1990.

[33] Reubroycharoen P, Vitidsant T, Asamic K, Yoneyama Y, Tsubaki N. Accelerated methanol synthesis in catalytically active supercritical fluid. Catal. Commun. 2003; 4(9) 461-464.

[34] Westerterp KR, Kuczynski M, Kamphuis CHM. Synthesis of methanol in a reactor system with interstage product removal. Ind. Eng. Chem. Res. 1989; 28 763-770.

[35] Kuczynski M, Oyevaar MH, Pieters RT, Westerterp KR. Methanol synthesis in a countercurrent gas-solid-solid trickle flow reactor, an experimental study. Chem. Eng. Sci. 1987; 42(8) 1887-1898.

[36] Haut B, Halloin V, Amor HB. Development and analysis of a multifunctional reactor for equilibrium reactions: Benzene hydrogenation and methanol synthesis Chem. Eng. Process. 2004; 43 979-986.

[37] Castier M, Rasmussen P, Fredenslund A. Calculation of simultaneous chemical and phase equilibria in nonideal systems. Chem. Eng. Sci. 1989; 44(2) 237-248.

[38] Hansen JB, Joensen F, editors. High conversion of synthesis gas into oxygenates. Proceeding of the NGCS; 1991; Oslo: Elsevier Science Publishers B.V.; 1990.

[39] Sorensen EL, Perregaard J. Condensing methanol synthesis and ATR - The technology choice for large-scale methanol production. Stud. Surf. Sci. Catal. 2004; 147 7-12.

[40] Topsoe HFA, Hansen JB. Method of preparing methanol. US5262443, United States 1993.

[41] Bennekom JG van, Venderbosch RH, Assink D, Lemmens KPJ, Winkelman JGM, Wilbers E, Heeres HJ. Methanol synthesis beyond chemical equilibrium. Chem. Eng. Sci. 2013; 87 204-208

[42] Poling BE, Prausnitz JM, O'Connel JP. The properties of gases and liquids. 5th ed. Singapore: McGraw-Hill; 2007.

[43] Mathias PM. A verstatile equilibrium equation of state. Ind. eng. Chem. Process Des. Dev. 1983; 22 385-391.

[44] Graaf GH, Sijtsema PJJM, Stamhuis EJ, Joosten GEH. Chemical equilibria in methanol synthesis. Chem. Eng. Sci. 1986; 41 2883-2890.

[45] Bennekom JG van, Winkelman JGM, Venderbosch RH, Nieland SDGB, Heeres HJ. Modeling and experimental studies on phase and chemical equilibria in high pressure methanol synthesis. Ind. Eng. Chem. Res. 2012; 51(38) 12233-12243

[46] Denise B, Sneeden RPA. Hydrocondensation of carbon dioxide: IV. J. Mol. Catal. 1982; 17 359-366.

[47] Smith KJ, Anderson RB. A chain growth scheme for the higher alcohols synthesis. J. Catal. 1984; 85(2) 428-436.

[48] Subramani V, Gangwal SK. A review of recent literature to search for an efficient catalytic process for the conversion of syngas to ethanol. Energy Fuels. 2008; 22 814-839.

[49] Davda RR. A review of catalytic issues and process conditions for renewable hydrogen and alkanes by aqueous-phase reforming of oxygenated hydrocarbons over supported metal catalysts. Appl. Catal., B. 2005; 56 171-186.

[50] Klier K, Chatikavanij V, Herman RG, Simmons GW. Catalytic synthesis of methanol from CO/H_2. IV. The effects of carbon dioxide J. Catal. 1982; 74 343-360.

[51] Forzatti P, Tronconi E, Pasquin I. Higher alcohol synthesis. Catal. Rev. Sci. Eng. 1991; 33(1&2) 109-168.

[52] Schubert M. Catalytic hydrothermal gasification of biomass - Salt recovery and continuous gasification of glycerol solutions. Zürich: ETH; 2010.

IntechOpen

IntechOpen